

# Chronostratigraphy of the *Hochterrassen* in the lower Lech valley (Northern Alpine Foreland)

Patrick Schielein, Gerhard Schellmann, Johanna Lomax, Frank Preusser, Markus Fiebig

## How to cite:

Schielein, P., Schellmann, G., Lomax, J., Preusser, F., & Fiebig, M. (2015): Chronostratigraphy of the *Hochterrassen* in the lower Lech valley (Northern Alpine Foreland). – E&G Quaternary Science Journal, 64 (1): 15–28. DOI: 10.3285/eg.64.1.02

## Abstract:

*Hochterrassen* (High or Higher Terraces) are a prominent geomorphological feature of the Northern Alpine Foreland and have traditionally been attributed to the Rissian glaciation. However, distinct morphological sublevels observed for this feature have often raised the question of their age. This issue is exemplarily investigated here on the *Langweider* and *Rainer Hochterrassen* in the lower Lech valley using different relative and numerical dating techniques. The lowest sublevel, the *Übergangsterrasse* is only preserved in small patches at the western rim of the *Rainer Hochterrasse* and is most probably of early Würmian age. The sublevel of the *Jüngere Hochterrasse* is older than the Last Interglacial, as indicated by luminescence ages of an overlying loess/palaeosol sequence and the development of a Luvisol on top of the terrace gravel. This terrace is composed of stacked gravel units that represent at least two accumulation phases correlating with Marine Isotope Stage (MIS) 6 for the top gravel and MIS 7 to MIS 10 (or older) for the basal gravel. It is not yet clear, if the deposition of the basal gravel unit corresponds to one or more aggradation phases during the Middle Pleistocene. The highest sublevel, the *Ältere Hochterrasse* also shows a composition of two stacked gravel units but so far, no numerical ages have been achieved for these units.

## Chronostratigraphie der Hochterrassen im unteren Lechtal (Nördliches Alpenvorland)

## Kurzfassung:

Hochterrassen sind eine im nördlichen Alpenvorland weit verbreitete geomorphologische Form, denen traditionell eine Entstehung während der Riss-Kaltzeit zugeordnet wird. Allerdings sind oftmals unterschiedliche Terrassenniveaus innerhalb der Hochterrassen zu beobachten, deren Altersstellung noch unbekannt ist. Dieses Thema wird hier am Beispiel der Langweider und Rainer Hochterrassen im unteren Lechtal mit Hilfe relativer und numerischer Datierungsmethoden untersucht. Das morphologisch tiefste Teilniveau, welches nur am westlichen Rand der Rainer Hochterrasse erhalten ist, stellt höchstwahrscheinlich eine frühwürmzeitliche Übergangsterrasse dar. Das nächsthöhere Niveau der Jüngeren Hochterrasse muss älter sein als das letzte Interglazial. Dafür sprechen die warmzeitliche Parabraunerde, die in Resten am Top des Terrassenkörpers erhalten ist, und die würmzeitliche Lösdeckschicht, welche durch Lumineszenzmessungen und Paläoböden datiert werden kann. Die Jüngere Hochterrasse besteht aus zwei gestapelten Kieskörpern, welche mindestens zwei Akkumulationsphasen zugeordnet werden können. Der hangende Kieskörper entstand während der Sauerstoff-Isotopenstufe (MIS) 6 und der liegende Kieskörper zwischen MIS 7 und MIS 10 (oder älter). Es ist jedoch nicht geklärt, in welcher Aufschüttungsperiode während des Mittelpleistozäns die Ablagerung des liegenden Kieskörpers stattfand. Das höchste Teilniveau, die Ältere Hochterrasse, zeigt auch eine Stapelung zweier Kieskörper, für diese liegen aber bisher keine numerischen Altersdaten vor.

## Keywords:

*Hochterrassen, Middle Pleistocene, Northern Alpine Foreland, fluvial terraces, luminescence dating*

**Addresses of authors:** P. Schielein, G. Schellmann, Department of Geography, University of Bamberg, Am Kranen 1, 96045 Bamberg, Germany. E-Mail: patrick.schielein@uni-bamberg.de; J. Lomax, Department of Geography, Justus-Liebig-University Giessen, Senckenbergstr. 1, 35390 Giessen, Germany. F. Preusser, Albert-Ludwigs-Universität Freiburg, Albertstr. 23-B, 79104 Freiburg i. Br., Germany. M. Fiebig, Institute of Applied Geology, University of Natural Resources and Life Sciences, Peter Jordan-Str. 70, A-1190 Vienna, Austria.

## 1 Introduction

The northern foreland of the Alps is characterised by prominent flights of fluvial terraces that are found parallel to most of the river systems. PENCK and BRÜCKNER (1901–1909) observed that some of these terraces are connected to terminal moraine ridges and concluded that the different terrace levels are representing glacial advances of different age. From this evidence, four glaciations of the foreland have been deduced, named (from old to young) Günzian, Mindelian, Rissian and Würmian. Later, two older glaciations, Danu-

bian (EBERL 1930) and Biberian (SCHAEFER 1957), have been inferred from river terraces located at higher levels. While for many decades this stratigraphic system has acted as global frame of reference, evidence from deep ocean sediments indicates that probably more glaciations occurred during the Quaternary than apparently observed in the Alps. The term *Hochterrasse* was introduced by PENCK (1884) to describe terraces that are situated 5 to 10 m above the valley floor. PENCK and BRÜCKNER (1901–1909) attributed all *Hochterrassen* to the Rissian, including those not linked to terminal moraines. Interestingly, in several valleys of the

northern Alpine Foreland, the *Hochterrasse* is subdivided into two or three levels (DOPPLER et al. 2011, references therein). This has led to the introduction of the term Rissian complex, but with controversy surrounding the question of how much time this complex may represent. Most probably the lowest *Hochterrassen* levels (“*Übergangsterrasse*” or *transitional terrace sensu* SCHELLMANN 1988; 2010) are of Early or Middle Würmian age, and the oldest *Hochterrassen* deposits have been accumulated quite likely during the third or fourth glaciation before present (Older and Middle Rissian *sensu* DOPPLER et al. 2011). Sometimes, equally elevated *Hochterrassen* deposits are composed of two separate gravel deposits with an interglacial fluvial facies at the base (e.g. “*Harterger Schichten*” in the Danube valley downstream of Regensburg (SCHELLMANN 1988; SCHELLMANN et al. 2010) and a cold climate *Hochterrassen* deposit *sensu stricto* at the top. The long duration of *Hochterrassen* formation and the various architectures of its deposits have to be taken into account when dating these units.

First attempts to date terrace deposits numerically were made in the middle of the 1990s using luminescence dating methods. At first, dating was focused on the age determination of the Last Glacial loess cover and its palaeosoils on top of *Hochterrassen* deposits in the Northern Alpine Foreland (e.g. MIARA 1996; BECKER-HAUMANN & FRECHEN 1997), which led to a penultimate glacial age estimation of the terrace gravels. FIEBIG & PREUSSER (2003) presented IRSL-data of the *Ingolstädter* and *Neuburger Hochterrassen* in the Danube valley and the *Rainer Hochterrasse* in the Lech valley with ages between 70 and 90 ka and concluded an aggradation of these terraces during the Early Würmian. Initial IRSL dating of *Hochterrassen* deposits from the valleys of Isar, Riss and Iller and from the Kirchner dry valley by KLASEN (2008) indicated ages between MIS 5e and MIS 6 when no fading correction was applied. When correcting these ages for fading, the *Hochterrassen* deposits would be associated with MIS 6–MIS 8. However, as results from fading tests were not straightforward, KLASEN (2008) emphasises the uncertain character of her IRSL ages. She also encountered difficulties dating the quartz fraction, due to instable signal components.

Therefore, a detailed chronology of the *Hochterrassen* deposits in the Northern Alpine Foreland is still lacking. Presented here, is a revised morphological and sedimentological subdivision of *Hochterrassen* in the lower Lech valley as well as a first set of numerical ages, derived from luminescence and ESR dating of the terrace gravels and overlying loess deposits. Thus, this study should provide first results and show the potential to date the *Hochterrassen* and their subdivisions in the lower Lech valley and beyond in the Northern Alpine Foreland.

## 2 Study area

The study area is located at the lower Lech valley downstream of Augsburg in the Northern Alpine Foreland (Fig. 1). The River Lech has its source in the Northern Calcareous Alps, breaks through the terminal moraines of Würmian and Rissian age and has cut its lower valley, up to 10 km in width, into Tertiary molasse and into the Early Pleistocene terrace flights of the *Iller-Lech-Schotterplatte*. In

the lower Lech valley, *Hochterrassen* with surfaces up to 20 m above the Late Quaternary valley floor are preserved. The latter is comprised of a sequence of Würmian *Niederterrassen* (Lower Terraces) and Holocene terraces.

In particular, the *Langweider Hochterrasse* is preserved west of the River Lech and further north the *Rainer Hochterrasse* is located east of the Lech. The *Langweider Hochterrasse* is bordered by the Late Quaternary Lech valley to the east and the Late Quaternary Schmutter valley to the west. SCHAEFER (1957) and others (SCHEUENPFLUG 1979, 1981; AKTAS & FRECHEN 1991) described the *Langweider Hochterrasse* as a uniform fluvial terrace level without any morphostratigraphic subdivision. However, differences in the petrographic composition of the gravel deposits of the *Langweider Hochterrasse* led to a subdivision into a base and a top unit by SCHAEFER (1957) and by AKTAS & FRECHEN (1991) in the southwest area of the *Langweider Hochterrasse* near the Schmutter valley. There, the base unit contains numerous quartzitic pebbles, whereas the top gravel exhibits a high amount of limestones of alpine origin. SCHEUENPFLUG (1979, 1981) assumed that the base unit is a periglacial gravel deposit of the Schmutter (“*periglazial-fluviatiler Schmutterschotter*”), whereas AKTAS & FRECHEN (1991) postulated a mixture of a Lech/Wertach and a Schmutter facies. Both studies agree in a deposition of the top unit by the River Lech. All mentioned studies assume a deposition of the top unit of the *Langweider Hochterrasse* during the Penultimate Glacial.

The *Rainer Hochterrasse* extends between the Late Quaternary Lech valley to the west and the Danube valley to the north. In the eastern part, the terrace is dissected by the Late Quaternary valley of the *Kleine Paar*. SCHAEFER (1966) subdivided the *Rainer Hochterrasse* morphostratigraphically into four terrace levels (Fig. 6), which developed due to the stepwise relocation of the Danube from the *Wellheimer Trockental* to the recent valley during the Middle Pleistocene (third-last to Penultimate Glacial). This subdivision of the *Rainer Hochterrasse* was largely rejected by KILIAN & LÖSCHER (1979) and TILLMANNS et al. (1982). Petrographic investigations by GRAUL (1943) and TILLMANNS et al. (1982) showed a high amount of Tertiary molasse sediments and reworked pebbles from older fluvial deposits in the eastern part, which were deposited by the *Kleine Paar*. In contrast, alpine limestones dominate the gravel of the western part, which they considered as a Lech facies. KILIAN & LÖSCHER (1979) found an elongated depression at the base of the gravel deposits of the *Rainer Hochterrasse*, which is orientated from SW to NE. Here, gravel thickness increases up to 15 m, whereas outside this depression gravel thickness reaches only up to 10 m. TILLMANNS et al. (1982), for the first time, postulated a subdivision of the gravel deposits of the *Rainer Hochterrasse* into a base and a top unit, which are separated by a horizon of loamy clods (“*Mergelbatzenhorizont*”) with both cold- and warm-climatic molluscs. Whereas previous studies assume an at least penultimate glacial age of the *Rainer Hochterrasse*, FIEBIG & PREUSSER (2003) presented first IRSL data of Early Würmian age. They dated three samples from sand lenses and layers inside the uniform *Hochterrassen* gravels in the area of the 7-m-*Hochterrasse* of SCHAEFER (1966) to  $75.5 \pm 7.3$  ka,  $80.2 \pm 9.7$  ka and  $84.1 \pm 5.7$  ka.

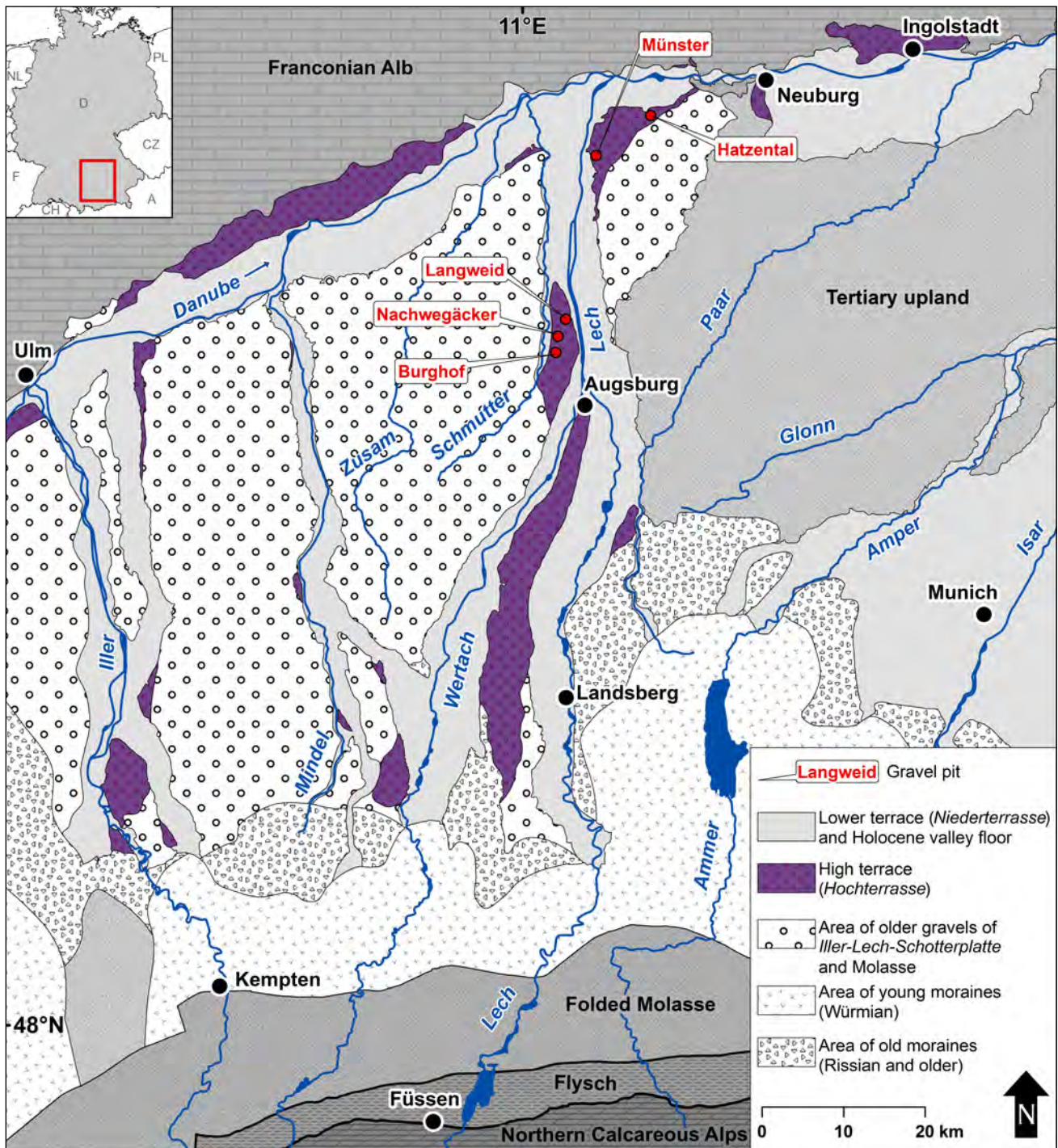


Fig. 1: Geological overview of the western part of the Bavarian Alpine Foreland. Hochterrassen with the location of outcrops mentioned in the text are accentuated. Modified after BAYERISCHES GEOLOGISCHES LANDESAMT (1996).

Abb. 1: Geologische Übersichtskarte des westlichen Bayerischen Alpenvorlands. Hochterrassen und die Lokationen der im Text aufgeführten Aufschlüsse sind hervorgehoben. Verändert nach BAYERISCHES GEOLOGISCHES LANDESAMT (1996).

### 3 Methods

The distribution and morphology of the Hochterrassen were surveyed by field mapping and high resolution Digital Elevation Models (LIDAR data, 2 x 2 m resolution) of the Bavarian State Office for Survey and Geoinformation (Munich). The sedimentology and pedology of the terraces and their cover layers was investigated in three outcrops on the Langweider Hochterrasse and in three outcrops on the Rain-er Hochterrasse (Fig. 1). For the determination of the matrix content, channel samples of 20 kg weight were taken from

different gravel units and the fine grain fraction (< 2 mm) was separated by sieving.

Moreover, drilling data from the Bavarian Environment Agency and from KILIAN & LÖSCHER (1979) were used for the reconstruction of gravel thickness and overlying aeolian deposits, and for the construction of a base map of the Quaternary deposits (Fig. 4 and 6).

Luminescence dating was carried out at the Institute of Applied Geology, University of Natural Resources and Life Sciences (Vienna). For determination of the equivalent dose ( $D_e$ ) quartz and feldspar grains (100–200  $\mu\text{m}$ )

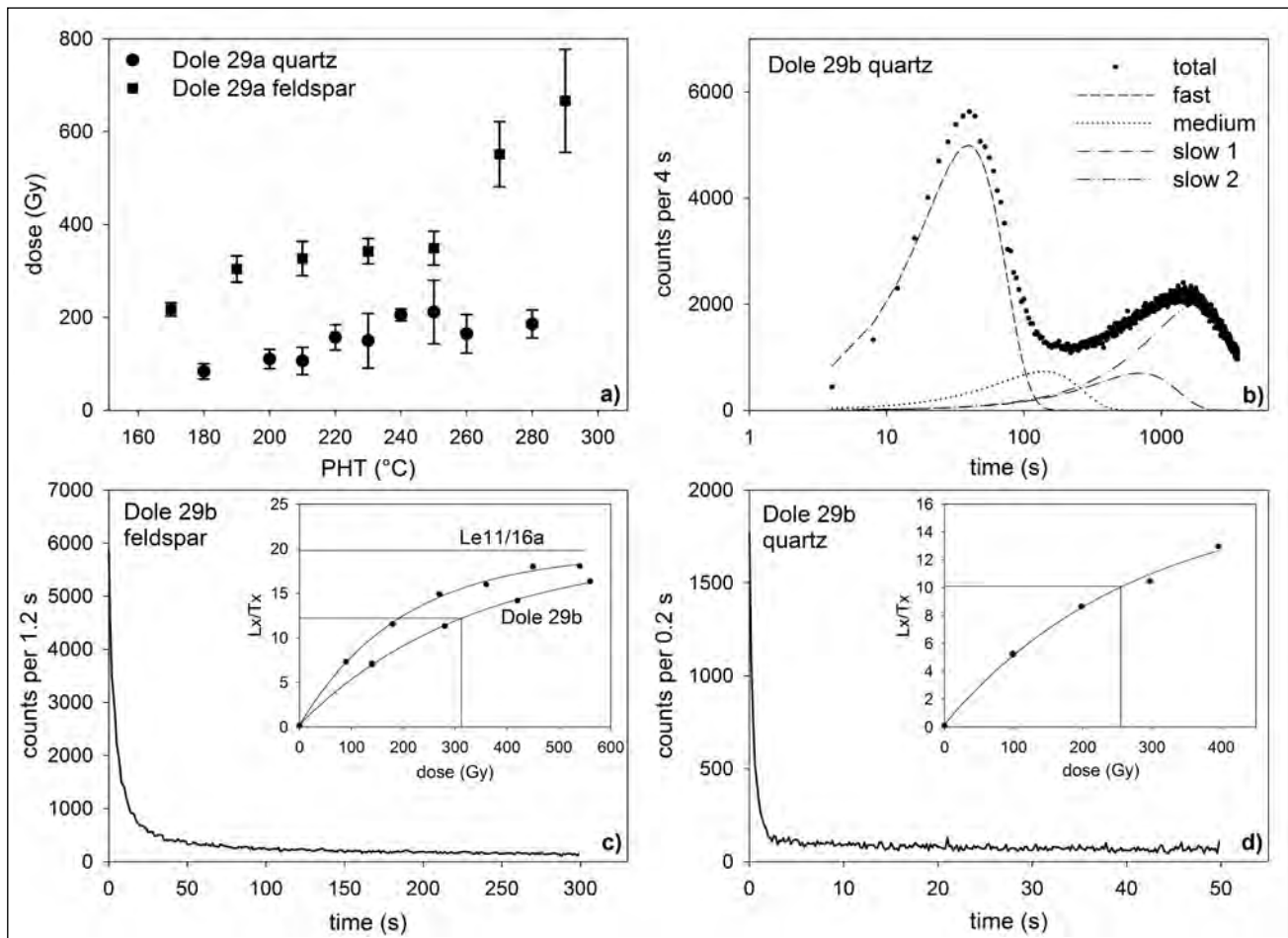


Fig. 2: Luminescence characteristics of the investigated samples. a) Preheat plateau tests of the quartz and feldspar fraction of sample Dole 29a. Both tests were conducted on 8mm discs, using five (quartz) or three (feldspar) aliquots per temperature. For the quartz measurements, the cutheat temperature was set to 20 °C below the preheat temperature (duration 10 s). For feldspar measurements, preheat and cutheat temperatures and durations (10 s) were the same. b) LM-OSL curve of quartz sample Dole 29b and component separation after CHOI et al. (2006). c) IRSL decay curve and growth curve of feldspar sample Dole 29b. The second growth curve is derived from sample Le11/16a, which showed signals near or above saturation. Both curves were fitted with a saturating exponential function, d) OSL decay curve and growth curve of quartz sample Dole 29b. The curve was fitted with a saturating exponential function.

Abb. 2: Lumineszenz-Charakteristika der untersuchten Proben. a) Vorheiz-Plateau-Tests der Quarz- und Feldspat-Fraktion der Probe Dole 29a. Beide Tests wurden an 8mm-Aliquots durchgeführt, mit jeweils fünf (Quarz) bzw. drei (Feldspat) Aliquots pro Temperaturschritt. Bei den Quarz-Messungen wurde die Cutheat-Temperatur auf 20 °C unterhalb der Vorheiztemperatur (Dauer 10 s) gesetzt. Bei den Feldspat-Messungen waren Vorheiz- und Cutheat-Temperatur und -dauer (10 s) identisch, b) LM-OSL-Kurve der Quarzprobe Dole 29b. Das Komponentensplitting wurde nach CHOI et al. (2006) durchgeführt, c) IRSL-Ausleuchtcurve und Wachstumskurve der Feldspatprobe Dole 29b. Die zweite Wachstumskurve stammt von der Feldspatprobe Le11/16a, welche Signale nahe und oberhalb der Sättigung zeigte. Beide Kurven wurden mit einer exponentiellen Sättigungsfunktion gefittet, d) OSL-Ausleuchtcurve und Wachstumskurve der Quarzprobe Dole 29b. Die Kurve wurde mit einer exponentiellen Sättigungsfunktion gefittet.

were extracted from the bulk sediment by physical and chemical laboratory treatment. Between 5 and 37 aliquots (mask size 1 or 2 mm, depending on signal intensity) were measured. Quartz standard measurements were carried out using the SAR protocol of MURRAY & WINTLE (2000, 2003). All measurements were conducted on Risø TL-DA-20 luminescence readers. For stimulation, blue LEDs were used and OSL-emission was filtered through an U340 filter (7.5 mm) For the feldspar fraction a modified SAR protocol following WALLINGA et al. (2000) and BLAIR et al. (2005) was applied including stimulation with IR diodes (50 °C for 300s) and signal detection through a 410 nm interference filter. Typical growth curves and OSL-/IRSL decay curves of the two mineral fractions are shown in Fig. 2c and 2d. Preheat temperatures for both quartz and feldspar were selected according to preheat plateau tests (Fig. 2a). Furthermore, a linear modulated OSL (LM-OSL)

measurement of one quartz sample (Dole 29b) was carried out, in order to investigate the proportion of OSL signal components (Fig. 2b). The measurement and curve separation followed CHOI et al. (2009), using a stimulation time of 3600s (divided into 900 channels of 4 s each), in which the power of the blue LEDs was increased from 0 to 90%. A preheat of 240 °C preceded the LM-OSL measurement, and the natural signal was measured. The LM-OSL curve and the separated components clearly indicate that the signal is dominated by the fast component. This is surprising, as many quartz samples from the northern alpine foreland show only a limited contribution of the fast component (e.g. KLASSEN 2008), and a thermally unstable medium component which may lead to age underestimation (LI & LI 2006, STEFFEN et al. 2009). In our case, this specific quartz sample seems appropriate to be measured with a standard SAR protocol.

U, Th, and K were determined by using laboratory gamma spectrometry on ~900 g of sample material. None of the samples showed signs of radioactive disequilibria in the uranium decay chain. The radionuclide concentrations were converted to dose rates by using conversion factors of ADAMIEC & AITKEN (1998). Cosmic dose rates were calculated based on geographic position and sampling depth below surface (PRESCOTT & HUTTON 1994). The coarse grain feldspar dose rates are based on an estimated internal K-concentration of  $12.5 \pm 1.5 \%$  (HUNTLEY & BARIL 1997). For sandy samples, water contents of  $10 \pm 7 \%$  were considered, for loess cover deposits a water content of  $15 \pm 7 \%$ .

The  $D_e$  was calculated using the central age model (CAM, GALBRAITH et al. 1999). One sample was tested for fading through a laboratory fading test and yielded a g-value of 3.3. We did not correct our samples for fading, because a) our samples are in the non-linear region of the growth curve, and b) acceptable agreement between quartz and uncorrected feldspar ages of aeolian deposits (DoLe/35) and of fluvial deposits from the Lech valley (SCHIELEIN & LOMAX 2013) in lower age ranges was observed. Still, the

risk of age underestimation by fading of the feldspar signal cannot be ruled out completely. A further concern in fluvial samples is incomplete bleaching, resulting in possible age overestimation. In the study of SCHIELEIN & LOMAX (2013), it was shown that incomplete bleaching may lead to ages, which are overestimated by a few ka when analysing polymineral fine grains, and by less than 1 ka when analysing coarse grain quartz in the same fluvial environment. These small residuals can be relevant for Holocene samples but the effect on Mid Pleistocene samples is likely to be small. The  $D_e$  determination of some of the luminescence samples from the *Langweider Hochterrasse* was challenging for other reasons. Here, quartz measurements did not yield any evaluable results due to very dim signals. Furthermore, the IRSL measurements of the oldest samples from the basal gravel unit (Le11/34c, Le11/34b, Le11/34a, Le11/16a) resulted in natural signals, of which the majority lay above all regenerated signals. This is shown for sample Le11/16a in Fig. 2c. These samples require further measurements in order to determine at least reliable minimum ages. At the current stage of the study, we can only consider these sam-

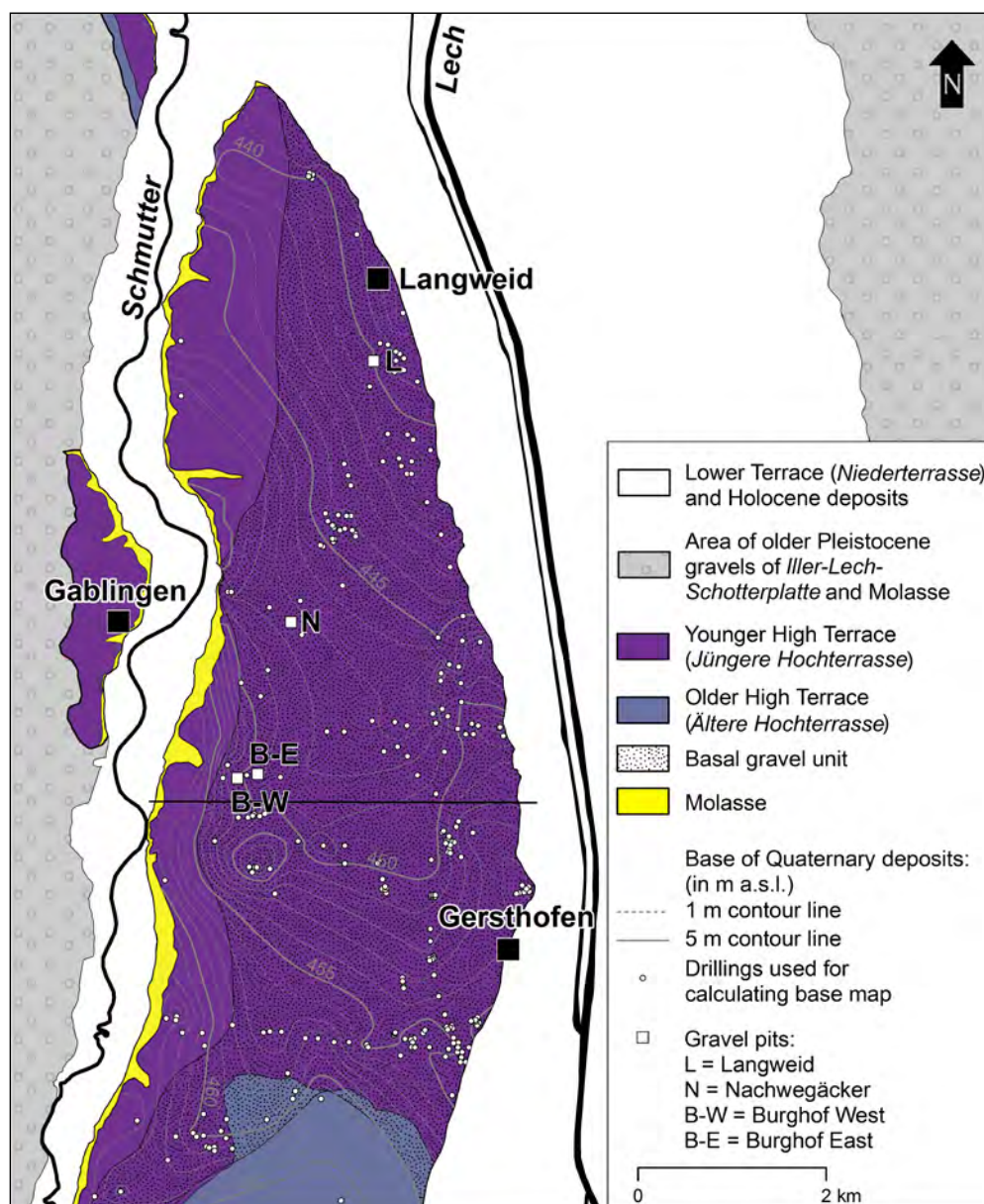


Fig. 3: The Langweider Hochterrasse - morphological subdivision, base of Quaternary deposits, distribution of basal gravel unit and location of outcrops. Stratigraphy of the Langweider Hochterrasse after SCHIELEIN & SCHELLMANN (c, d, in prep.) and SCHELLMANN (a, b, in prep.). The black line indicates the approximate position of the geological cross section (Fig. 8)

Abb. 3: Die Langweider Hochterrasse – morphologische Gliederung, Quartärbasis, Verbreitung des Sockelschotters und Lage der Aufschlüsse. Stratigraphie der Langweider Hochterrasse nach SCHIELEIN & SCHELLMANN (c, d, in prep.) und SCHELLMANN (a, b, in prep.). Die schwarze Linie gibt die ungefähre Lage des geologischen Querprofils (Abb. 8) an.

ples to be older than the samples from the top gravel unit and possibly older than other samples from the basal gravel unit, due to their comparatively high natural signals.

One mollusc shell from a loamy clod inside the base unit of the *Langweider Hochterrasse* was dated by Electron Spin Resonance (ESR). The ESR measurements were conducted at the University of Cologne. The mollusc shell was ground to a particle diameter between 125 and 250 µm. 10 aliquots with a weight of 0.022 g were gamma-irradiated by a <sup>60</sup>Co source with dose rates between 17.8 and 445 Gy. ESR intensity was measured using a Bruker ESP 300E spectrometer. The measurement parameters were: 25 mW microwave power, 0.19 G modulation amplitude, 20.972 s sweep time, 40 G scan width, and an accumulation of 30 scans. The D<sub>e</sub> value was determined using the program 'fit-sim' by GRÜN (version 1993) and age calculation was carried out with the program Data V.6' by GRÜN (version 1999). The U content of the mollusc shell (0.79 ppm) and the U (2.61 ppm), Th (7.25 ppm) and K (0.97 %) content of the surrounding sediments were determined via ICP-MS at the University of Cologne. The measured water content of the loam lense was 27 %, for the age calculations a water content of 25 ± 5 % was used. For the unlikely case of linear uranium assimilation and higher water contents, the ESR-age would increase.

## 4 Results

### 4.1 *Langweider Hochterrasse*

The *Langweider Hochterrasse* can morphologically be subdivided into two differently elevated levels (Fig. 3): a higher and therefore older terrace level in the southern part (*Ältere Hochterrasse*) and an approximately 2 m lower level

(*Jüngere Hochterrasse*) in the central and northern part (cf. SCHIELEIN & SCHELLMANN d, accepted; SCHELLMANN a, accepted). The latter is exposed in several outcrops, whereas no outcrops are present in the area of the *Ältere Hochterrasse*. Concerning the elevation of the base of the fluvial gravel deposits, no differences between both terraces exist. An elongated depression with maximum thickness of fluvial gravel deposits is cut in the Tertiary molasse and is distributed both under the older and the younger level of the *Langweider Hochterrasse* (Fig. 3). In contrast to previous research, which assumed a uniform gravel deposition in most parts of the *Langweider Hochterrasse*, several outcrops in the area of the elongated depression exhibit a subdivision of the fluvial gravel deposits of the *Langweider Hochterrasse*. Here, a well-sorted sandy basal unit with a thickness of up to 10 m is overlain by a coarse gravelly top unit with a thickness between 4 and 8 m. The basal unit is restricted to the area of the elongated depression (Fig. 3).

The subdivision of the *Langweider Hochterrasse* into two sediment units is well exposed in the gravel pit Langweid, which is situated in the northern part of the *Langweider Hochterrasse* near the eastern terrace rim (Fig. 3). Here, the aeolian cover layer of the terrace was anthropogenically removed. The outcrop stretches over a length of more than 50 m, is 8 m high and shows a distinct division of two stacked gravel units in a depth of c. 4–5 m below the surface of the terrace gravels (Fig. 4). The top unit is composed of poorly sorted medium and coarse gravels in a sandy matrix, whereas layers of skeletal (grain-supported) gravels frequently occur. This unit has a relatively low amount of sand and is horizontally and trough bedded. In contrast, the underlying gravel unit predominantly consists of medium gravels and granules, is rich in sand, well sorted and



Fig. 4: The structure of the *Langweider Hochterrasse* in the gravel pit Langweid: The top gravel unit is horizontal and trough bedded, whereas the basal gravel unit is large-scale cross bedded and appears lighter in colour, due to the higher content of sand. Length of the rule in the center is 3 m. See Fig. 3 for location of the outcrop.

Abb. 4: Der Aufbau der *Langweider Hochterrasse* in der Grube Langweid: Der hangende Kieskörper ist horizontal und trogförmig kreuzgeschichtet, während der liegende Kieskörper großbogig schräggeschichtet ist. Letzterer erscheint wegen des höheren Sandanteils heller. Die Länge des Zollstocks in der Bildmitte beträgt 3 m. Zur Lage des Aufschlusses siehe Abb. 3.

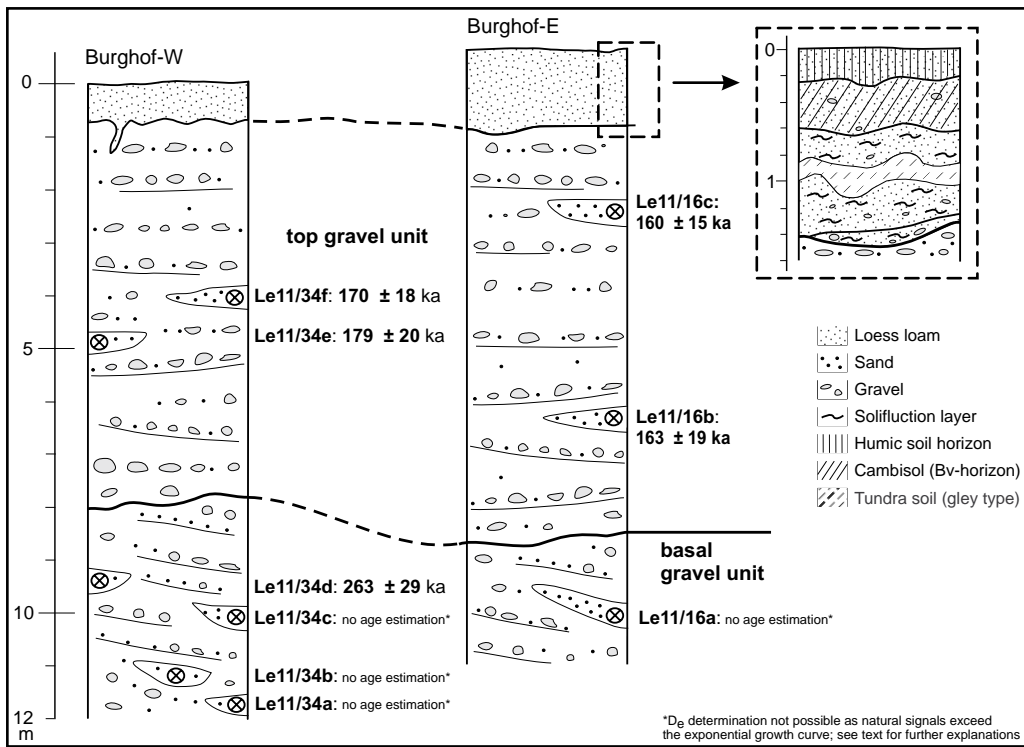


Fig. 5: Outcrops Burghof W (left) and Burghof E (right) on the Langweider Hochterrasse. See Fig. 3 for location of the outcrops.

Abb. 5: Aufschlussprofile in der Kiesgrube Burghof W (links) und Burghof E (rechts) auf der Langweider Hochterrasse. Zur Lage der Aufschlüsse siehe Abb. 3.

large-scale cross bedded (Fig. 4). This basal unit appears lighter coloured, due to the higher content of sand.

#### 4.1.1 Gravel pits Burghof West and East

The gravel pits Burghof West and East, in the western part of the *Langweider Hochterrasse*, show a similar structure of the fluvial sediments and their cover layers. In both outcrops, the gravelly *Hochterrasse* deposits are covered by an up to 1.5 m thick layer of sandy loess loam, on which a Holocene cambisol is developed (Fig. 5). In the central part of the sandy loess loam, a *Nassboden* (tundra soil of gley type) of most probably Pleniglacial Würmian age is preserved. At the base of this aeolian sediment cover, solifluction layers, composed of reworked loess loam and terrace gravels, are present.

The *Hochterrasse* gravels are divided into two units (Fig. 5). A top unit with a thickness of 6 to 8 m is composed of horizontal and slightly trough-bedded medium and coarse gravel layers containing many cobbles and boulders up to 30 cm in diameter. In this unit, gravel layers free of matrix are common, whereas sand lenses suitable for luminescence dating are hardly present. The basal unit of predominantly sand-rich medium gravel layers is exposed above the groundwater table with thicknesses of 2 to 4 m. This unit is partially trough-, and sometimes large-scale cross bedded. The sand content is considerably higher than in the top gravel unit. In the gravel pit Burghof East, the basal unit has a matrix content of about 40 % by weight, in contrast to the top unit with a matrix content of only c. 16 % by weight.

IRSL dating of four sand lenses from the top unit yielded results consistent within uncertainties (Fig. 5, Table 1). The ages of  $160 \pm 15$  ka (Le11/16c),  $163 \pm 19$  ka (Le11/16b),  $170 \pm 18$  ka (Le11/34f), and  $179 \pm 20$  ka (Le11/34e) give strong evidence for a deposition during the Penultimate Glaciation (MIS 6).

From the basal sand rich gravel unit, five sand lenses were measured by IRSL. One sand lense in the gravel pit Burgheim E yielded an IRSL age of  $263 \pm 29$  ka (Le11/34d) indicating a deposition between MIS 7 and 8 (Fig. 5, Table 1). IRSL measurements of three further samples from sand lenses in the basal gravel unit (Le11/34c, Le11/34b, Le11/34a) and the sample Le11/16a from the basal gravel unit at the location Burghheim W yielded many natural signals above the growth curve. Therefore,  $D_e$  determination and age estimations were not possible. It may only be assumed that these deposits are older than the top gravel unit and possibly older than sample Le11/34d. Overall, the dating results give clear evidence that the basal gravel unit, which is distributed in the elongated depression, is older than the Penultimate Glaciation (MIS 6). A clear assignment to marine isotope stages is difficult though, due to the large errors, and closeness to the upper age limit of the technique. Most probably, the deposition took place between MIS 7 and 9, but the saturated luminescence signals of the lower most parts of the basal gravel unit may also indicate deposition during an older isotope stage.

#### 4.1.2 Gravel pit Nachwegäcker

In the gravel pit Nachwegäcker, c. 2 km north of the location Burghof (Fig. 3), both the Würmian cover layer and the top unit of the *Hochterrasse* gravel were mostly removed by quarrying. Only at one part of the gravel pit, both gravel units with similar sediment characteristics as in the gravel pits described above were exposed. From the basal gravel unit, shells of *Succinea putris* (genus determination by W. Rähle, Stuttgart State Museum of Natural History), embedded in a loamy clod in a depth of c. 11 m below surface, could be dated by ESR (Table 1: Le11/26c). This land snail lives in wet environments such as river banks and marshes and can occur both in glacial and interglacial periods

Tab. 1: Measurement details of dosimetric samples.

Tab. 1: Messwerte der dosimetrischen Proben.

Sample	Sampling locations (Gauss – Krüger coordinates)	Depth (m)	Grain size ( $\mu\text{m}$ )	Radionuclide concentrations <sup>a</sup>			Cosmic dose rate (Gy/ka)	Water content (%)	Dose rate (Gy/ka)	n <sup>b</sup>	D <sub>e</sub> (Gy) <sup>c</sup>	Age (ka)
				K (%)	U (ppm)	Th (ppm)						
DoLe35 (OSL)	4419240	0.5	150-200	0.61	1.35	2.92	0.21 $\pm 0.03$	10 $\pm$ 7	1.20 $\pm 0.09$	37	23.7 $\pm 2.60$	19.8 $\pm$ 2.7
DoLe35 (IRSL)	5389934			$\pm 0.01$	$\pm 0.03$	$\pm 0.09$			1.87 $\pm 0.18$		7	36.0 $\pm 2.20$
DoLe37 (IRSL)	4419240 5389934	2.5	150-200	1.35 $\pm 0.02$	3.19 $\pm 0.05$	9.28 $\pm 0.26$	0.16 $\pm 0.02$	10 $\pm$ 7	3.32 $\pm 0.30$	20	314 $\pm 25$	95 $\pm$ 12
DoLe29a (OSL)	4418973	4.0	150-200	0.51	0.98	1.54 $\pm$	0.13 $\pm$ 0.02	10 $\pm$ 7	0.87 $\pm$ 0.05	38	242 $\pm$ 36	279 $\pm$ 45
DoLe29a (IRSL)	5390961			$\pm 0.01$	$\pm 0.03$	0.07			1.52 $\pm$ 0.14		39	400 $\pm$ 20
DoLe29b (OSL)	4418973	4.0	150-200	0.49	1.01	1.59 $\pm$	0.13 $\pm$ 0.02	10 $\pm$ 7	0.87 $\pm$ 0.05	40	253 $\pm$ 41	291 $\pm$ 51
DoLe29b (IRSL)	5390961			$\pm 0.01$	$\pm 0.03$	0.07			1.52 $\pm$ 0.14		37	333 $\pm$ 36
Le11/34a (IRSL)	4414268 5367668	11.5	100-200	0.98 $\pm 0.02$	2.00 $\pm 0.04$	4.77 $\pm$ 0.16	0.05 $\pm$ 0.01	10 $\pm$ 7	2.25 $\pm$ 0.18	5	... <sup>d</sup>	no age estimation <sup>d</sup>
Le11/34b (IRSL)	4414251 5367667	11	100-200	0.76 $\pm 0.01$	0.50 $\pm 0.01$	1.61 $\pm$ 0.06	0.06 $\pm$ 0.01	10 $\pm$ 7	1.49 $\pm$ 0.13	5	... <sup>d</sup>	no age estimation <sup>d</sup>
Le11/34c (IRSL)	4414275 5367670	10	100-200	0.90 $\pm 0.01$	0.41 $\pm 0.01$	1.39 $\pm$ 0.06	0.07 $\pm$ 0.01	10 $\pm$ 7	1.59 $\pm$ 0.15	4	... <sup>d</sup>	no age estimation <sup>d</sup>
Le11/34d (IRSL)	4414265 5367652	9.5	100-200	0.48 $\pm 0.01$	1.06 $\pm 0.02$	1.77 $\pm$ 0.07	0.07 $\pm$ 0.01	10 $\pm$ 7	1.39 $\pm$ 0.14	5	367 $\pm$ 18	263 $\pm$ 29
Le11/34e (IRSL)	4414175 5367672	5	100-200	0.61 $\pm 0.01$	1.22 $\pm 0.03$	1.97 $\pm$ 0.09	0.12 $\pm$ 0.02	10 $\pm$ 7	1.60 $\pm$ 0.16	5	287 $\pm$ 13	179 $\pm$ 20
Le11/34f (IRSL)	4414145 5367670	4.0	100-200	0.63 $\pm 0.01$	0.70 $\pm 0.02$	1.45 $\pm$ 0.06	0.13 $\pm$ 0.02	10 $\pm$ 7	1.48 $\pm$ 0.15	5	252 $\pm$ 9	170 $\pm$ 18
Le11/16a (IRSL)	4414399 5367771	10.0	100-200	0.72 $\pm 0.01$	0.73 $\pm 0.01$	1.49 $\pm$ 0.06	0.07 $\pm$ 0.01	10 $\pm$ 7	1.50 $\pm$ 0.13	4	... <sup>d</sup>	no age estimation <sup>d</sup>
Le11/16b (IRSL)	4414399 5367771	6.5	100-200	0.45 $\pm 0.01$	1.30 $\pm 0.02$	1.61 $\pm$ 0.06	0.10 $\pm 0.01$	10 $\pm$ 7	1.44 $\pm$ 0.13	10	235 $\pm$ 18	163 $\pm$ 19
Le11/16c (IRSL)	4414399 5367771	2.5	100-200	0.70 $\pm 0.01$	0.49 $\pm 0.01$	1.58 $\pm$ 0.06	0.16 $\pm 0.02$	10 $\pm$ 7	1.51 $\pm$ 0.13	10	242 $\pm$ 10	160 $\pm$ 15
Le11/26c (ESR)	4414665 5369303	11	125-250	0.97 $\pm$ 0.1 <sup>e</sup>	0.79 $\pm$ 0.1 (shell) 2.61 $\pm$ 0.1 <sup>e</sup>	7.25 $\pm$ 0.1 <sup>e</sup>	0.052 $\pm$ 0.02	25 $\pm$ 5 <sup>e</sup>	0.889 $\pm$ 0.065	10	191.8 $\pm$ 21.9	204 $\pm$ 27

<sup>a</sup> K = Potassium, U = Uranium, Th = Thorium

<sup>b</sup> n = Amount of measured aliquots

<sup>c</sup> For all samples, the CAM (central age model, Galbraith et al. 1999) was used for De-determination.

<sup>d</sup> D<sub>e</sub> determination was not possible as natural signals exceed the exponential growth curve. See text for further explanations.

<sup>e</sup> Data of the surrounding sediment.



(LOŽEK 1965). The snail (Le11/26c) yielded an ESR age of  $204 \pm 27$  ka. This age indicates a deposition of the basal gravel unit during MIS 6, or 7.

#### 4.2 Rainer Hochterrasse

A morphostratigraphic subdivision of the *Rainer Hochterrasse* as presented by SCHAEFER (1966) could not be confirmed for the most parts. Only the increase of the surface elevation between his 7- and 14-m- *Hochterrasse* could be verified (Fig. 6), as already stated by KILIAN & LÖSCHER (1979). Here, we assume a morphological subdivision into a *Jüngere Hochterrasse* (JHT) and a *Ältere Hochterrasse* (ÄHT). The latter includes the 14- and 21-m-*Hochterrasse* of

SCHAEFER (1966), whereas the JHT covers his 7-m-*Hochterrasse*. Moreover, at the western part of the *Rainer Hochterrasse*, small patches of a 2 m lower elevated and therefore younger terrace, are distributed in the area of the town of Rain and in the western part of the gravel pits near Münster (Fig. 6). This terrace was designated by SCHAEFER (1966) as *Neuburger-Tal-Terrasse*, but in the following, the term “*Übergangsterrasse (ÜT)*” (SCHELLMANN 1988) is used for this terrace due to its significantly lower surface level.

The *Rainer Hochterrasse* can be sedimentologically divided into two stacked gravel units. The base of the fluvial gravel deposits of the *Rainer Hochterrasse* shows no difference between the JHT and the ÄHT. The course of contour lines in the Quaternary base map (Fig. 6) traces an elongat-

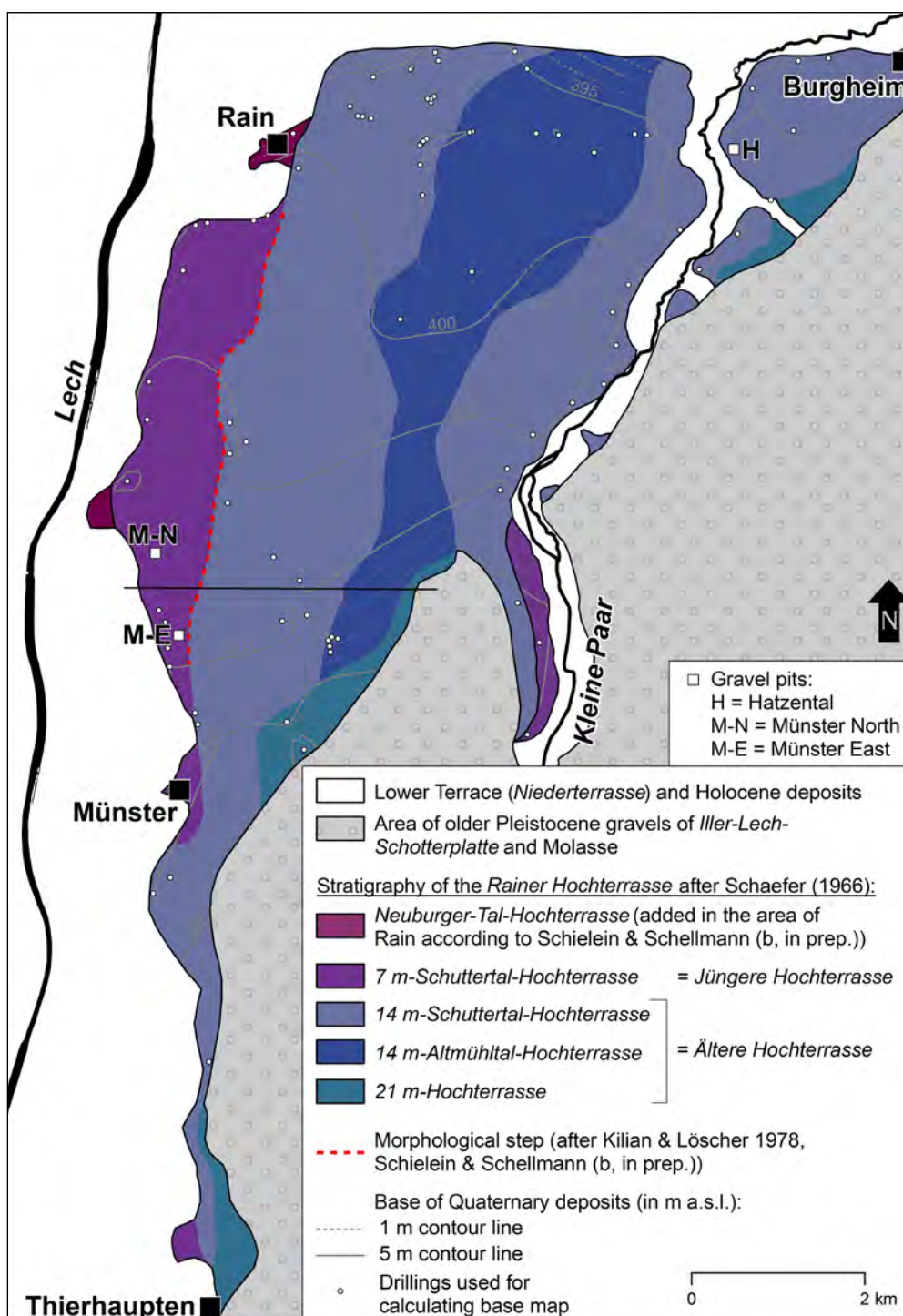


Abb. 6: The *Rainer Hochterrasse* – morphological subdivision (including interpretation of SCHAEFER 1966), base of Quaternary deposits and location of outcrops. The black line indicates the approximate position of the geological cross section (Fig. 8).

Abb. 6: Die *Rainer Hochterrasse* – morphologische Gliederung (einschließlich der Interpretation durch SCHAEFER 1966), Quartärbasis und Lage der Aufschlüsse. Die schwarze Linie gibt die ungefähre Lage des geologischen Querprofils (Abb. 8) an.

ed depression with a maximum thickness of 15 m of Quaternary deposits. This depression and its orientation from SW to NE beneath the *Rainer Hochterrasse* was already mentioned by KILIAN & LÖSCHER (1979). In the following section, we present sedimentological and chronological results from the gravel pits Münster N and Münster E, both located in the area of the *JHT*. First on-site inspections of the gravel pit Hatzental (Fig. 6) confirm the division of the *Rainer Hochterrasse* into two stacked gravel units also for the area of the *ÄHT*. Here, a trough- and horizontal bedded top unit of medium and coarse gravels with a relatively low matrix content exhibits a thickness of c. 4 m and is underlain by a basal gravel unit, which is composed of large-scale cross bedded fine to coarse gravels and is strikingly rich in sand.

#### 4.2.1 Münster N

The gravel pit Münster N exhibits the extensively distributed cover layer of the *Rainer Hochterrasse*, a sandy loess with a thickness of more than 1 m. In the upper part, a tundra soil strangled by cryoturbations, is prevalent. In the lower part, the fine-grained loess deposit contains single gravels, due to solifluidal reworking (Fig. 7).

Beneath the loess cover, at the top of the *Hochterrassen* gravel, a fossil Bt-horizon of an interglacial luvisol is preserved that most probably represents the Last Interglacial (Eemian). Cones of this fossil soil can reach to a depth of 1 m into the gravel. The gravel in the outcrop is separated into two units by an unconformity. The top gravel unit is comprised of medium and coarse gravels in a sandy matrix and shows horizontal and trough-bedding. At the top of this unit, cryoturbations of the gravel layers can occur. Beneath the unconformity, the basal gravel unit composed of large-scale cross bedded fine to coarse gravels with a high content of sandy matrix in some places contains coarse and medium sand layers with thicknesses of up to 1 m. In the

investigated profile, one sand layer extends over a width of 30 m, was clearly laterally bedded and passes into the sandy gravels of the underlying gravel unit.

The sand layer at the top of the base gravel unit was sampled twice for luminescence dating. Quartz and feldspar minerals yielded ages between  $219 \pm 31$  ka and  $291 \pm 51$  ka (Tab. 1, Fig. 7: DoLe29a/b). Two OSL-ages ( $291 \pm 51$  ka,  $279 \pm 45$  ka) and one IRSL-age ( $263 \pm 27$  ka) indicate a deposition of the base unit during MIS 8 or MIS 9, and one feldspar age ( $219 \pm 31$  ka) points to MIS 7. However, the uncertainties on the luminescence ages are large, hence a clear assignment to an isotope stage remains difficult.

#### 4.2.2 Münster E

The outcrop Münster E is situated in a periglacial trough, cut into the gravel of the *Rainer Hochterrasse* over a width of c. 20 m. The trough is filled with fine-grained cover sediments up to a thickness of 2.5 m (Fig. 7). In the upper part, the cover layer equates to the outcrop Münster N, comprising of sandy loess with a fossil tundra soil and a solifluction layer. Below, a stack of two humus zones (*Humuszonen*) is preserved. The upper humus zone is 40 cm thick, of brownish colour and contains several gravels, as it is partly strangled with the overlying solifluction layer. The lower humus zone is c. 1 m thick, dark grey-brown and shows light brown blotches in the upper part. Both humus zones are comparable to the Early Würmian *Mosbacher Humuszonen* (SCHÖNHALS et al. 1964, SEMMEL 1968) and were accumulated by aeolian transport and slope wash of soil sediments under dry conditions. The blotched layer correlates most probably to the “*gefleckter Horizont*” of ROHDENBURG (1964) and might have developed under acidic conditions by bleaching along plant roots. In contrast, SEMMEL (1996) interpreted these light brown blotches as initial soil browning beneath an Early Würmian coniferous forest steppe.

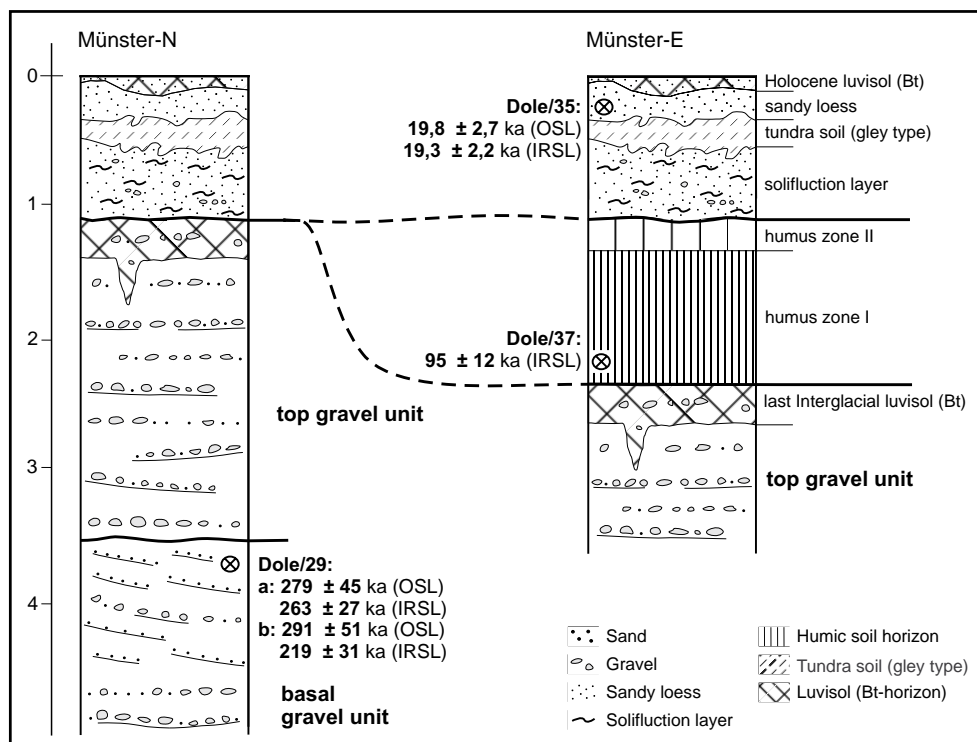


Fig. 7: Outcrops Münster N (left) and Münster E (right) on the *Rainer Hochterrasse*. See Fig. 6 for location of the outcrops.

Abb. 7: Aufschlussprofile in der Kiesgrube Münster N (links) und Münster E (rechts) auf der *Rainer Hochterrasse*. Zur Lage der Aufschlüsse siehe Abb. 6.

At the top of the gravels of the *Rainer Hochterrasse*, the preserved Bt-horizon of a luvisol of most probably Eemian age, reaches a thickness of up to 1 m in cones. The gravel itself is exposed over a length of more than 100 m and exhibits a distinct separation of two stacked units in some parts. A separation by a layer of loamy clods (“*Mergelbatzen-horizont*”) as presented by TILLMANN et al. (1982) was not comprehensible during the survey. Only single loamy clods in both gravel units were noticed. The top gravel unit is horizontally and trough-bedded and dominated by medium and coarse gravels in a sandy matrix. In places, layers of skeletal gravels occur. The basal gravel unit is only partially exposed and sometimes shows large-scale cross bedding. The sand content is considerably higher than in the top gravel unit.

In the outcrop Münster E, the cover deposits contain typical Würmian soils and humus zones. This assignment is confirmed by luminescence dating (Fig. 7: DoLe35 & DoLe37). The sandy loess near the surface yielded ages (DoLe-35) of  $19.8 \pm 2.7$  ka (OSL) and  $19.3 \pm 2.2$  ka (IRSL), and the lower humus zone an age of  $95 \pm 12$  ka (DoLe-37, IRSL). So far, no luminescence dating results from both units of the *Hochterrassen* gravels in the pit Münster E have been achieved. However, due to the interglacial soil at the top

of the terrace gravels and the dating results of the cover layer, the deposition of the *Hochterrassen* gravels before the Eemian Interglacial is assured.

## 5 Discussion

The *Langweider Hochterrasse* and the *Rainer Hochterrasse* are composed of two different terrace levels (*Jüngere* and *Ältere Hochterrasse*). The *Rainer Hochterrasse* additionally features some small patches of Early Würmian age (*Übergangsterrasse*) at the western terrace rim. The examined *Hochterrassen* feature both in the areas of the *JHT* and in the areas of the *ÄHT* a basal gravel unit, which can be clearly distinguished from the top gravel unit by sedimentological characteristics (Fig. 8). The elongated depression at the base of the *Langweider* and the *Rainer Hochterrasse* indicates a continuous distribution of a basal gravel unit beneath the top gravel unit in the area of the *JHT* as well as in the area of the *ÄHT*.

In other areas of the Northern Alpine Foreland, *Hochterrassen* can also be morphologically subdivided (e.g. DOPPLER et al. 2011). The *Dillinger Hochterrasse* in the Danube valley upstream of the Lech-Danube confluence is supposed to be comprised of up to four terraces accord-

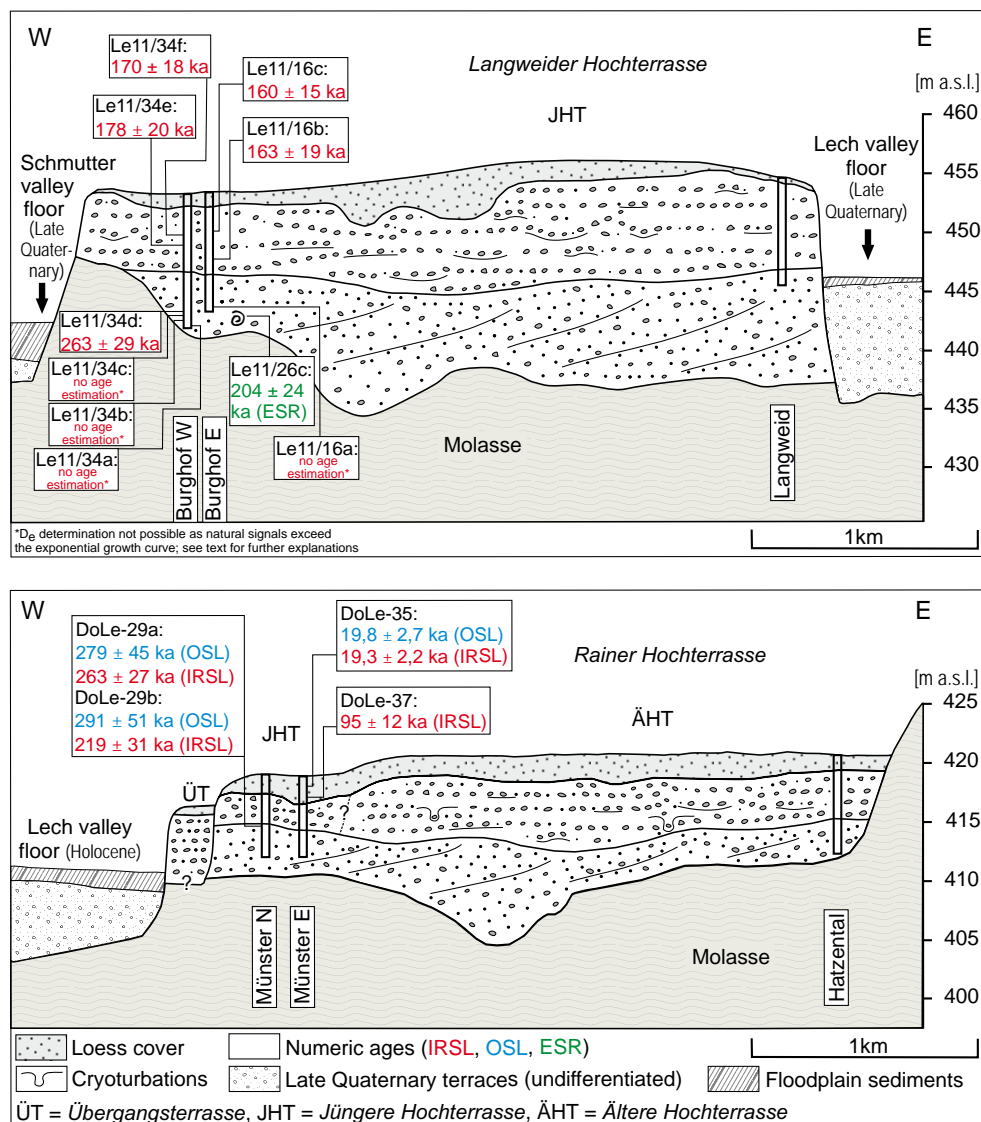


Fig. 8: Geological cross sections through the Langweider Hochterrasse (top) and the Rainer Hochterrasse (bottom) showing the vertical subdivision of the terraces in a top and a basal gravel unit and all numerical age evidences. See Fig. 3 and Fig. 6 for approximate position of the cross sections. All outcrops and the *Übergangsterrasse* (at the edge of the Rainer Hochterrasse) were projected into the cross sections.

Abb. 8: Geologisches Querprofil durch die Langweider Hochterrasse (oben) und durch die Rainer Hochterrasse (unten) mit der vertikalen Aufteilung in einen hangenden und einen liegenden Kieskörper und allen numerischen Altershinweisen. Zur ungefähren Lage der Querprofile siehe Abb. 3 und Abb. 6. Alle Aufschlüsse und die *Übergangsterrasse* (am Rand der Rainer Hochterrasse) wurden in die Querprofile projiziert.

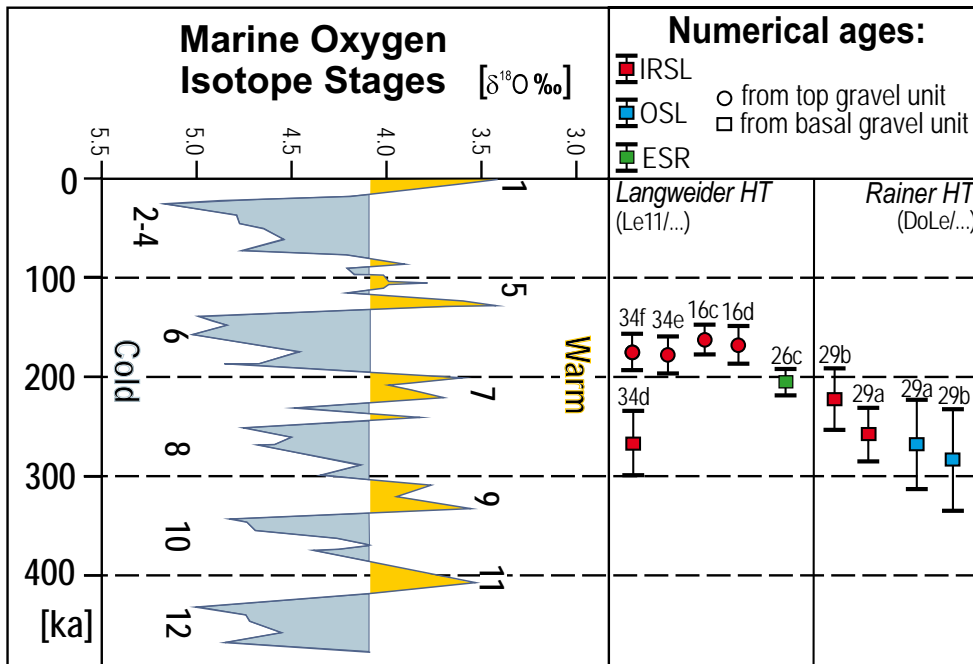


Fig. 9: Numerical ages of the Langweider Hochterrasse and Rainer Hochterrasse compared to Marine Isotope Stages.

Abb. 9: Die numerischen Alter aus der Langweider Hochterrasse und Rainer Hochterrasse im Vergleich zu den marinen Sauerstoff-Isotopenstufen.

ing to different authors (GRAUL 1962, LEGER 1988, BIBUS & STRAHL 2000). BIBUS & STRAHL (2000) correlate each individual terrace unit of the *Dillinger Hochterrasse* with one glacial period between the Penultimate and the fifth-last Glacial. Also, the *Hochterrasse* of the Danube near Straubing can be divided into three terrace levels (SCHELLMANN 1988, SCHELLMANN et al. 2010). In the Riß valley, two *Hochterrassen* levels are well-defined (MIARA 1996, BIBUS & KÖSEL 1997). For all mentioned *Hochterrassen* levels, numerical ages are not available. A stacking of two different gravel units as it could be found inside the *Rainer* and *Langweider Hochterrasse* was also presented for the *Hochterrassen* of the Danube near Straubing (SCHELLMANN 1988, SCHELLMANN et al. 2010) and for the *Hochterrassen* in northern Switzerland (GRAF 2009), but again without the application of numerical dating methods.

In the present study, numerical ages of the different sedimentological subdivisions of *Hochterrassen* in the lower Lech valley are available for the first time. Here, a temporal difference between the deposition of two stacked gravel units during the Middle Pleistocene and the correlation of at least two distinctive accumulation periods with Marine Isotope Stages was verified (Fig. 9). The top gravel units of the *Rainer* and *Langweider Hochterrasse* in the area of the *Jüngere Hochterrasse* were most probably both deposited during MIS 6. The feldspar ages from the top gravel unit of the *Langweider Hochterrasse* are in agreement with the Würmian age of the loess cover layer and with the assignment of the fossil Bt-horizon at the top of the gravels to the Last Interglacial in the gravel pit Münster on the *Rainer Hochterrasse*. This contrasts IRSL ages of FIEBIG & PREUSSER (2003) from the same gravel pit, which yielded Early Würmian ages of the *Hochterrasse*. As the gravel pit covers a great area for some decades and is situated at the western border of the *Jüngere Hochterrasse* (Fig. 6) it might also have covered parts of the *Übergangsterrasse*. The samples of FIEBIG & PREUSSER (2003) could be derived from this *Übergangsterrasse*, which is most probably of Early Würmian age, but this question still needs to be clarified.

A longer hiatus exists between the deposition of the basal and the top unit. Dating results indicate a deposition at least during MIS 7 for the basal unit. Older depositional phases, inter- or lateglacial deposition environments, and multiphase accumulation cannot be ruled out for the basal gravel unit, but the luminescence ages obtained for this unit are too imprecise for a more detailed reconstruction of terrace deposition. In the outcrop Münster N (*Rainer Hochterrasse*), the feldspar and the quartz ages yield ages between MIS 7 and 9. Probably, the basal gravel units of both *Hochterrassen* correlate with each other, due to their composition of sand-rich, well sorted gravels and their similar bedding structure. This is confirmed by an IRSL-age of fluvial sands and an ESR-age of a snail inside the basal gravel unit of the *Langweider Hochterrasse*. An assumption of a late- or even interglacial deposition is supported by the observed trough- and large-scale cross bedding of the basal gravel unit, which reminds of the bedding of the Holocene gravels in the Lech valley upstream of Augsburg (GESSLEIN & SCHELLMANN 2011, GESSLEIN 2013). Interglacial gravel units at the base of a *Hochterrasse* were also found in the Danube valley near Regensburg, namely the *Hartinger Schichten*, which contain interglacial peat (SCHELLMANN 1988, 2010).

## 6 Conclusion

The *Langweider* and *Rainer Hochterrasse* in the lower Lech valley were deposited in multiple accumulation phases. Both examined terraces can be morphologically subdivided in a younger (*JHT*) and an older terrace level (*ÄHT*). Furthermore, two accumulation phases are documented by two stacked gravel units with different sedimentological characteristics inside one morphological terrace. Luminescence dating proved the chronological differentiation of the gravel units and their correlation to MIS 6 (top gravel), and to MIS 7 or older (basal gravel), respectively. Thereby, it is not yet clear, in which aggradation period during the Middle Pleistocene the basal gravel was deposited. Its large-scale cross bedding supports an inter- or late glacial deposition.

In general, dating Middle Pleistocene deposits with OSL and IRSL of the quartz and the feldspar fraction, respectively, remains a challenge due to approaching signal saturation. Therefore, for future research, different luminescence dating techniques should be taken into account as well as ESR-dating of molluscs and of sedimentary quartz in order to be able to compare the reliability and accuracy of different dating methods. Beside the use of numerical geochronological methods for dating *Hochterrassen* deposits in the Northern Alpine Foreland, traditional geomorphological and geological methods (e.g. mapping of morphological units, sedimentology, palaeosoils in loess cover layers) are essential for relative and absolute age evidences of terrace aggradation and therefore always have to be considered.

## 7 Acknowledgements

We appreciate the financial and technical support of the study provided by the Bavarian Environment Agency in the framework of the EU-funded project “*Informationsoffene Oberflächennahe Geothermie*”.

We like to thank Dr. W. Rähle for genus determination of the ESR dated gastropods, and Prof. Dr. U. Radtke (Cologne) for the ESR measurements.

## References

- ADAMIEC, G. & AITKEN, M. (1998): Dose-rate conversion factors: update. – *Ancient TL*, 16: 37–50.
- AKTAS, A. & FRECHEN, M. (1991): Mittel- bis jungpleistozäne Sedimente der Hochterrassen in der nördlichen Iller-Lech-Platte. – Sonderveröffentlichungen des Geologischen Instituts der Universität zu Köln, 82: 19–41; Köln.
- BAYERISCHES GEOLOGISCHES LANDESAMT (1996): Geologische Karte von Bayern 1:500.000. München.
- BECKER-HAUMANN, R. & FRECHEN, M. (1997): Vergleichende Lumineszenzdatierungen mit IRSL und TL am Deckschichtenprofil Bobingen / Lechtal. – *Zeitschrift geologischer Wissenschaften*, 25 (5/6): 617–633.
- BIBUS, E. & KÖSEL, M. (1997): Paläoböden und periglaziale Deckschichten im Rheingletschergebiet von Oberschwaben und ihre Bedeutung für Stratigraphie, Reliefentwicklung und Standort. – *Tübinger Geowissenschaftliche Arbeiten*, D3: 89 p.; Tübingen.
- BIBUS, E. & STRAHL, M. (2000): Zur Gliederung und Altersstellung der bayerischen Hochterrassen nördlich des Donauniedes. – *Zeitschrift für Geomorphologie*, N.F., 44 (2): 211–232.
- BLAIR M.W., YUKIHARA, E.G. & MCKEEVER, S.W.S. (2005): Experiences with single aliquot OSL procedures using coarse-grain feldspars. – *Radiation Measurements*, 39: 361–374.
- DOPPLER, G., KROEMER, E., WALLNER, J., JERZ, H. & GROTTENTHALER, W. (2011): Quaternary Stratigraphy of Southern Bavaria. – *E&G Quaternary Science Journal*, 60 (2-3): 329–365.
- EBERL, B. (1930): Die Eiszeitenfolge im nördlichen Alpenvorlande – Ihr Ablauf, ihre Chronologie auf Grund der Aufnahme im Bereich des Lech- und Illergletschers. – 427 S.; Augsburg.
- FIEBIG, M. & PREUSSER, F. (2003): Das Alter fluvialer Ablagerungen aus der Region Ingolstadt (Bayern) und ihre Bedeutung für die Eiszeitenchronologie des Alpenvorlandes. – *Zeitschrift für Geomorphologie*, N.F., 47 (4): 449–467.
- GALBRAITH, R.F., ROBERTS, R.G., LASLETT, G.M., YOSHIDA, H. & OLLEY, J.M. (1999): Optical dating of single and multiple grains of quartz from Jinnium rock shelter, northern Australia: Part I, experimental design and statistical models. – *Archaeometry*, 41: 339–364.
- GRAF, H. R. (2009): Stratigraphie von Mittel- und Spätpleistozän in der Nordschweiz. Beiträge zur Geologischen Karte der Schweiz, 168. – Wabern (Bundesamt für Landestopografie swisstopo).
- GESSELEIN, B. (2013): Zur Stratigraphie und Altersstellung der jungquartären Lechterrassen zwischen Hohenfurch und Kissing unter Verwendung hochauflösender Airborne-LiDAR-Daten. – *Bamberger Geographische Schriften – Sonderfolge*, 10. 165 S.
- GESSELEIN, B. & SCHELLMANN, G. (2011): Jungquartäre Flussterrassen am mittleren Lech zwischen Kinsau und Klosterlechfeld – Erste Ergebnisse. – *E&G Quaternary Science Journal*, 60 (4): 400–413.
- GRAU, H. (1943): Zur Morphologie der Ingolstädter Ausräumungslandschaft. Die Entwicklung des unteren Lechlaufes und des Donaumoosbodens. – *Forschungen zur deutschen Landeskunde*, 43: 1–114.
- GRAU, H. (1962): Eine Revision der pleistozänen Stratigraphie des schwäbischen Alpenvorlandes. – *Petermanns Geographische Mitteilungen*, 106: 253–271.
- HUNTLEY, D.J. & BARIL, M.R. (1997): The K content of K-feldspars being measured in optical and thermo-luminescence dating. – *Ancient TL*, 15: 11–13.
- KILLIAN, R. & LÖSCHER, M. (1979): Zur Stratigraphie des Rainer Hochterrassen-Schotters östlich des unteren Lechs. – *Sammlung quartärmorphologischer Studien II*, Heidelberger Geographische Arbeiten, 49: 210–217.
- KLASEN, N. (2008): Lumineszenzdatierung glazifluvialer Sedimente im nördlichen Alpenvorland. – *Inaugural-Dissertation*, Universität zu Köln: 209 S.; Köln.
- LEGER, M. (1988): Géomorphologie de la vallée subalpine du Danube entre Sigmaringen et Passau. – *Thèse du doctorat*, Univ. Paris VII: 621 S.; Paris.
- LI, B. & LI, S.-H. (2006): Comparison of De estimates using the fast component and the medium component of quartz OSL. – *Radiation Measurements*, 41: 125–136.
- LOŽEK, V. (1965): Das Problem der Lößbildung und die Lößmollusken. – *Eiszeitalter und Gegenwart*, 16: 61–75.
- MIARA, S. (1996): Deckschichtenuntersuchungen zur Gliederung der Rißeiszeit beiderseits der Iller im Gebiet des Rhein- und Illergletschers (westliches Alpenvorland, Deutschland). – *Jahresberichte und Mitteilungen des oberrheinischen geologischen Vereins*, N.F., 78: 359–374.
- MURRAY A.S. & WINTLE, A.G. (2000): Luminescence dating using an improved single-aliquot regenerative-dose protocol. – *Radiation Measurements*, 32: 57–73.
- MURRAY, A.S. & WINTLE, A.G. (2003): The single aliquot regenerative dose protocol: potential for improvements in reliability. – *Radiation Measurements*, 37: 377–381.
- PENCK, A. (1884): Ueber Periodicität der Thalbildung. – *Verhandlungen der Gesellschaft für Erdkunde*, XI: 39–59; Berlin.
- PENCK, A. & BRÜCKNER, E. (1901–1909): Die Alpen im Eiszeitalter. – 3 Bde.: 1199 S.; Leipzig.
- PRESCOTT, J.R. & HUTTON, J.T. (1994): Cosmic ray contributions to dose rates for luminescence and ESR dating: large depth and long-term time variations. – *Radiation Measurements*, 23: 497–500.
- ROHDENBURG, H. (1964): Ein Beitrag zur Deutung des „Gefleckten Horizonts“. – *Eiszeitalter und Gegenwart*, 15: 66–71.
- SCHAEFER, I. (1957): Geologische Karte von Augsburg und Umgebung 1:50.000 mit Erläuterungen. – *Bayerisches Geologisches Landesamt*, 92. S.; München.
- SCHAEFER, I. (1966): Der Talknoten von Donau und Lech. – *Mitteilungen der Geographischen Gesellschaft München*, 51: 59–111.
- SCHELLMANN, G. (1988): Jungquartäre Talgeschichte an der unteren Isar und der Donau unterhalb von Regensburg. – *Inaugural-Dissertation* Universität Düsseldorf; Düsseldorf.
- SCHELLMANN, G. (2010): Neue Befunde zur Verbreitung, geologischen Lagerung und Altersstellung der würmzeitlichen (NT1 bis NT3) und holozänen (H1 bis H7) Terrassen im Donautal zwischen Regensburg und Bogen. – *Bamberger Geographische Schriften*, 24: 1–77.
- SCHELLMANN, G. (a, in prep.): Quartärgeologische Karte 1:25.000 des Schmutter- & Lechtals auf Blatt Nr. 7530 Gablingen mit Erläuterungen – Kartierungsergebnisse aus dem Jahr 2011. – *Bamberger Geographische Schriften*.
- SCHELLMANN, G. (b, in prep.): Quartärgeologische Karte 1:25.000 des Schmutter- & Lechtals auf Blatt Nr. 7430 Wertingen mit Erläuterungen – Kartierungsergebnisse aus dem Jahr 2011. – *Bamberger Geographische Schriften*.
- SCHELLMANN, G., IRMLER, R. & SAUER, D. (2010): Zur Verbreitung, geologischen Lagerung und Altersstellung der Donauterrassen auf Blatt L7141 Straubing. – *Bamberger Geographische Schriften*, 24: 89–178.
- SCHUEENPFLUG, L. (1979): Die risszeitliche Hochterrasse des Lechs nördlich Augsburg und die Schmutter (Bayerisch Schwaben). – *Heidelberger Geogr. Arb.*, 49: 194–209.
- SCHUEENPFLUG, L. (1981): Die Schotterfazies des Augsburgers Umlandes. – *Berichte des Naturwissenschaftlichen Vereins für Schwaben e.V.*, 85 (1/2): 14–21, Augsburg.

- SCHIELEIN, P (2012): Jungquartäre Flussgeschichte des Lechs unterhalb von Augsburg und der angrenzenden Donau. – Bamberger Geographische Schriften – Sonderfolge, 9. 150 S.
- SCHIELEIN, P & LOMAX, J. (2013): The effect of fluvial environments on sediment bleaching and Holocene luminescence ages – A case study from the German Alpine Foreland. *Geochronometria* 40 (4), 283–293.
- SCHIELEIN, P. & SCHELLMANN, G. (a, in prep.): Quartärgeologische Karte 1:25.000 des Lech- und Donautals auf Blatt Nr. 7231 Genderkingen mit Erläuterungen – Kartierungsergebnisse aus den Jahren 2008 bis 2009. – Bamberger Geographische Schriften.
- SCHIELEIN, P. & SCHELLMANN, G. (b, in prep.): Quartärgeologische Karte 1:25.000 des Lechtals auf Blatt Nr. 7331 Rain mit Erläuterungen – Kartierungsergebnisse aus den Jahren 2008 bis 2009. – Bamberger Geographische Schriften.
- SCHIELEIN, P. & SCHELLMANN, G. (c, in prep.): Quartärgeologische Karte 1:25.000 des Lechtals auf Blatt Nr. 7431 Thierhaupten mit Erläuterungen – Kartierungsergebnisse aus dem Jahr 2011. – Bamberger Geographische Schriften.
- SCHIELEIN, P. & SCHELLMANN, G. (d, in prep.): Quartärgeologische Karte 1:25.000 des Lechtals auf Blatt Nr. 7531 Gersthofen mit Erläuterungen – Kartierungsergebnisse aus dem Jahr 2011. – Bamberger Geographische Schriften.
- SCHÖNHALS, E., ROHDENBURG H. & SEMMEL, A. (1964): Ergebnisse neuerer Untersuchungen zur Würmlößgliederung in Hessen. – *Eiszeitalter und Gegenwart*, 15: 199–206.
- SEMMEL, A. (1968): Studien über den Verlauf jungpleistozäner Formung in Hessen. – *Frankfurter Geographische Hefte*, 45: 133 S., Frankfurt.
- SEMMEL, A. (1996): Paläoböden im Würmlöß, insbesondere im Altwürmlöß des Steinbruchs Mainz-Weisenau - Problemstellung und Übersicht über die Forschungsergebnisse. – *Frankfurter Geowissenschaftliche Arbeiten*, D 20: 11–20.
- STEFFEN, D., PREUSSER, F. & SCHLUNEGGER, F. (2009): OSL quartz age underestimation due to unstable signal components. – *Quaternary Geochronology*, 4 (5): 353–362.
- TILLMANN, W., MÜNZING, K., BRUNNACKER, K. & LÖSCHER, M. (1982): Die Rainer Hochterrasse zwischen Lech und Donau. – *Jahresberichte und Mitteilungen des oberrheinischen geologischen Vereins*, N. F., 64: 79–99.
- WALLINGA, J., MURRAY, A.S. & WINTLE, A.G. (2000): The single-aliquot regenerative-dose (SAR) protocol applied to coarse-grain feldspar. – *Radiation Measurements*, 32: 529–533.